

See discussions, stats, and author profiles for this publication at: <https://www.researchgate.net/publication/282726046>

# Sorption studies of Cs<sup>+</sup>, Ba<sup>2+</sup>, and Co<sup>2+</sup> ions on bentonite using radiotracer, ToF-SIMS, and XRD techniques

Article *in* Radiochimica Acta · January 2001

CITATIONS

6

READS

5

2 authors:



Talal Shahwan

Birzeit University

55 PUBLICATIONS 1,571 CITATIONS

SEE PROFILE



H. N. Erten

Bilkent University

75 PUBLICATIONS 1,047 CITATIONS

SEE PROFILE

Some of the authors of this publication are also working on these related projects:



Use of electrospun fiber mats for the remediation of hypersaline geothermal brine [View project](#)



مقالات حول النشر العلمي [View project](#)

# Sorption studies of Cs<sup>+</sup>, Ba<sup>2+</sup>, and Co<sup>2+</sup> ions on bentonite using radiotracer, ToF-SIMS, and XRD techniques

By T. Shahwan and H. N. Erten\*

Department of Chemistry, Bilkent University, 06533 Bilkent, Ankara, Turkey

(Received March 8, 2001; accepted May 25, 2001)

*Sorption / Cs / Ba / Co / Bentonite / ToF-SIMS*

**Summary.** The sorption behaviour of Cs<sup>+</sup>, Ba<sup>2+</sup>, and Co<sup>2+</sup> ions on bentonite were investigated using the radiotracer method, Time of Flight-Secondary Ion Mass Spectroscopy (ToF-SIMS), and X-Ray Diffraction (XRD). The sorption of Cs<sup>+</sup> and Ba<sup>2+</sup> were exothermic while sorption of Co<sup>2+</sup> was endothermic. The sorption data were well described by Freundlich and Dubinin–Radushkevich isotherms. According to ToF-SIMS results Na<sup>+</sup> and Mg<sup>2+</sup> were the primary exchanging ions in bentonite. The XRD spectra showed that no structural changes were associated with the sorption of Cs<sup>+</sup> and Co<sup>2+</sup>, and BaCO<sub>3</sub> precipitate was formed upon the sorption of Ba<sup>2+</sup> on bentonite.

## Introduction

The geological disposal of radioactive wastes is considered as an appropriate means of isolation of potentially hazardous radionuclides from the human environment. The geological disposal of radioactive wastes is composed of natural and engineered barriers that are expected to retard the radionuclides migration effectively. The engineered barriers consist of canister, overpack, and backfill materials. Bentonite, by virtue of its outstanding sorption properties, has been chosen as one of the most promising candidates to be used as a backfill material [1]. <sup>137</sup>Cs (*t*<sub>1/2</sub> = 30.1 y) is a fission product that is produced in high yield and due to its long half life is a principal radiocontaminant. <sup>140</sup>Ba (*t*<sub>1/2</sub> = 14.8 d) is also a fission product with a high yield. Ba being a homolog of Ra is a suitable element for the radiochemical study of Ra, which have several radioisotopes that are important in radioactive waste considerations. <sup>60</sup>Co (*t*<sub>1/2</sub> = 5.3 y) is formed by activation of <sup>59</sup>Co in nuclear materials. <sup>60</sup>Co is widely used for medical applications.

In this study, radiotracer batch experiments were carried out to examine the effects of time, concentration, and temperature on the sorption of Cs<sup>+</sup>, Ba<sup>2+</sup>, and Co<sup>2+</sup> on bentonite. The radionuclides <sup>137</sup>Cs, <sup>133</sup>Ba, and <sup>60</sup>Co were used as radiotracers. These experiments provided information about the kinetics, sorption isotherms, and the thermodynamic parameters such as enthalpy change,  $\Delta H^\circ$ , entropy change,  $\Delta S^\circ$ , and Gibbs free energy change,  $\Delta G^\circ$ , in sorption. Since

sorption is mainly a surface phenomenon, part of our sorption studies were carried out using the surface sensitive technique Time of Flight-Secondary Ion Mass Spectrometry (ToF-SIMS). In addition, depth profiling up to 70 Å was done using ToF-SIMS to investigate Cs<sup>+</sup>, Ba<sup>2+</sup>, and Co<sup>2+</sup> concentrations throughout the clay surface. ToF-SIMS studies were performed to examine the surface composition of bentonite prior to and after sorption. As a result, quantification of the depletion of different elements initially contained within the analyzed clay surface enabled the evaluation of the role of ion exchange in the sorption process. X-Ray Diffraction (XRD) was used to study the mineralogical composition of the natural bentonite samples. XRD spectra of the clay samples following sorption provided information about the possible structural changes taking place in the clay lattice.

## Experimental

The natural clay minerals used were obtained from the Turkish Mining Institute (MTA). They originated from Giresun region situated in the north eastern Anatolia, on the Black Sea coast. The particle size of bentonite used throughout the study was < 38 µm.

### FTIR analysis of natural clay samples

The FTIR analysis of bentonite was carried out using a Bomem MB-Series instrument. The samples were introduced using KBr pellets and spectra were recorded in the range 400–4000 cm<sup>-1</sup>. The scan rate was 22 scans/minute, the resolution 4 cm<sup>-1</sup> and a total of 64 scans were recorded for each spectrum. A Win Bomem Easy software was used to process the results.

### I – Radiotracer experiments

The batch method was used, and prior to the sorption experiments pretreatment of the clay samples was carried out. This pretreatment step was intended to mimic the equilibrium existing between the natural clays and groundwater. Aliquots of 30 mg of the clay were introduced into pre-weighed tubes, and 3 ml of Bilkent tapwater, as substitute for groundwater, were added into each tube which were then shaken

\*Author for correspondence (E-mail: erten@fen.bilkent.edu.tr).

for 4 days with a lateral shaker at 125 rpm. The cation composition of Bilkent tapwater was determined by FAAS. The average concentration (meq/ml) of  $\text{Na}^+$ ,  $\text{K}^+$ ,  $\text{Mg}^{2+}$ , and  $\text{Ca}^{2+}$  were  $3.92 \times 10^{-4}$ ,  $1.04 \times 10^{-4}$ ,  $4.30 \times 10^{-4}$ , and  $3.24 \times 10^{-4}$ , respectively. Samples were then centrifuged at 6000 rpm for 30 minutes and the liquid phases were discarded. Each tube was then weighed to determine the small amount of water remaining ( $\Delta W_{\text{pt}}$ ).

In all the radiotracer experiments, shaking was done in a temperature-controlled environment using a Nuve ST 402 water bath shaker equipped with a microprocessor thermostat. A Spectrum 88 type instrument equipped with a High Purity Germanium Coaxial Detector connected to a multi-channel analyzer was used in activity measurement. All the experiments were performed in duplicates. The relative error in activity stemming from adsorption by inside tube surface was determined to be less than  $\pm 0.05$ . Tubes were shaken vigorously prior to centrifugation to collect any liquid drops or clay particles adhering to the inside surface/cover of the tube. To avoid any contamination by the clay particles following centrifuging of tubes, 2 ml of the supernatant solution (out of the 3 ml initial volume in each tube) was carefully separated and then counted. The uncertainties associated with the measurements stemmed principally from those of counting statistics. Other minor error sources were those from weight and volume measurements. Considering all sources, the percentage error in the  $R_d$  values was calculated to be less than  $\pm 10\%$  in all cases.

### Effect of time of contact

To each of the clay samples, 3 ml portions of  $\text{Cs}^+$ ,  $\text{Ba}^{2+}$ , or  $\text{Co}^{2+}$  solutions were added. The initial concentration of each solution was  $1 \times 10^{-3}$  meq/ml prepared from  $\text{CsCl}$ ,  $\text{BaCl}_2$ , and  $\text{Co}(\text{NO}_3)_2$  salts, spiked with  $^{137}\text{Cs}$ ,  $^{133}\text{Ba}$ , and  $^{60}\text{Co}$  radiotracers, respectively. Samples were shaken at room temperature for periods ranging from half an hour to seven days. They were then centrifuged and 2 ml portions of the liquid phases were counted to determine their activities.

### Effect of loading and temperature

Loading experiments were carried out to investigate the effect of initial cesium, barium, and cobalt ion concentrations on sorption at different temperatures. The experiments were performed at the initial concentrations of  $1 \times 10^{-3}$ ,  $1 \times 10^{-4}$ ,  $1 \times 10^{-5}$ , and  $1 \times 10^{-6}$  (meq/ml) at four different temperatures; 30, 40, 50 and 60 °C. Three ml portions of solutions containing appropriate amounts of radiotracers were added to each sample tube containing 30 mg of clay. Prior to mixing, the solutions and clays were heated to the desired temperature. The samples were then shaken for two days, centrifuged and 2 ml portions of the liquid phase were counted.

## II – ToF-SIMS and XRD experiments

Bentonite samples weighing 4.0 g each were exposed to 400.0 ml aliquots of 0.010 M  $\text{CsCl}$ , or 0.010 M  $\text{BaCl}_2$ , or 0.010 M  $\text{Co}(\text{NO}_3)_2$  and mixed for 48 hours using a magnetic stirrer. Samples were then filtrated and dried overnight at 90 °C. The measured pH ranged from 6.97 to 8.23 and no external pH control was done.

### ToF-SIMS analysis of clays

ToF-SIMS analysis of natural and Cs-, Ba-, and Co-exchanged bentonite powder samples were performed using a Vacuum Generator ToF-SIMS instrument located at the University of Bristol Interface Surface Analysis Centre. During analysis, the vacuum in the analysis chamber was kept at approximately  $10^{-9}$  mbar. Spectra were recorded over fifty accumulations, at  $\times 5000$  magnification, *i.e.* an area of  $64 \times 48$  mm. The ion beam pulse length was 30 ns with a repetition rate of 10 kHz. The  $\text{Ga}^+$  ion gun used to produce the ions was operated at 1 nA current and 20 keV energy. The electron flood gun was used as required for neutralization. These conditions resulted in an etching rate of approximately 10 Å per 50 second etch. The samples were etched and analysis performed at successive depths of 10, 20, 30, 40, 50, and 70 Å.

### XRD analysis of clays

A Bruker AXS D500 X-ray diffractometer was used to analyze powder samples of natural-, Cs-, Ba-, and Co-sorbed bentonite. The source consisted of unfiltered  $\text{Cu } K_\alpha$  radiation, generated in a tube operating at 40 kV and 30 mA. Spectra were recorded with 2 theta values ranging from 3 to 35 degrees in steps of 0.02 degree and dwell times of 10 s per step. The samples were rotated during analysis, which was performed at ambient temperature. Bruker AXS DIFFRAC-AT software was used to process the results and compare them with the Joint Committee on Powder Diffraction Standards (JCPDS) database.

## Results and discussion

### Characterization of natural bentonite

The XRD analysis showed that the main components of natural bentonite were montmorillonite in addition to quartz, feldspars and some calcite as shown in Fig. 6a. The IR spectrum of natural bentonite is given in Fig. 1. The broad OH stretching feature at  $3623 \text{ cm}^{-1}$  is typical for montmorillonite. This band forms the overall envelope for a wide range of  $\text{AlAlOH}$  and  $\text{AlMgOH}$  environments in the highly substituted and distorted structure. Other characteristic bands are

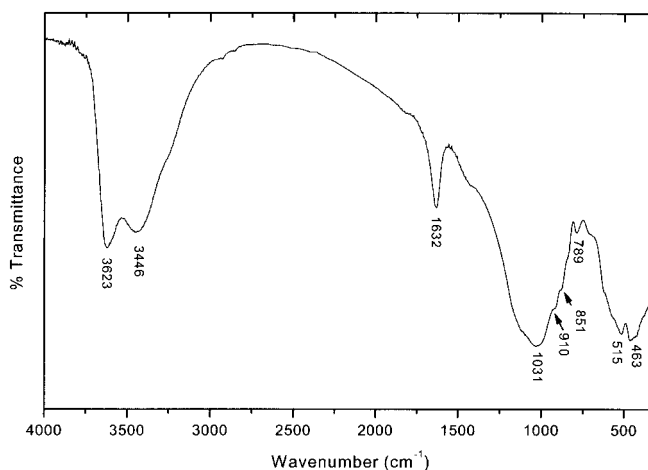


Fig. 1. IR spectrum of natural bentonite.

the OH deformation bands near 915 cm<sup>-1</sup> (AlAlOH) and the 840 cm<sup>-1</sup> (AlMgOH) [2].

### The radiochemical studies

The results were expressed in terms of the distribution ratio,  $R_d$ , defined as the ratio of sorbed cation concentration on the solid phase to that in the liquid phase, and given by the equation:

$$R_d = \frac{VA^\circ - (V + \Delta W_{pt})A_1}{A_1 W_s} \quad (1)$$

Where  $A^\circ$  and  $A_1$  are the count rates of solution prior to and following sorption (cps)/ml,  $W_s$  is the weight of solid material (g), and  $\Delta W_{pt}$  is the amount of liquid remaining in the tube after pretreatment, prior to sorption. The variation of  $R_d$  of sorbed Cs<sup>+</sup>, Ba<sup>2+</sup>, and Co<sup>2+</sup> on bentonite as a function of sorption time indicate a fast sorption process. Sorption was very fast during the first few hours of contact time. This was followed by a slower process where some desorption occurred leading finally to equilibrium in about two days of contact.

Loading experiments were carried out to investigate the effect of initial cation concentration on sorption at various temperatures. The loading curves were constructed by plotting the  $R_d$  values versus  $\log[C]_s$ , where the latter refers to the equilibrium concentration of sorbed cations on bentonite (meq/g). The resulting curves for each sorbed ion at  $T = 303$  K are illustrated in Fig. 2. The curves show characteristic inverse S shape indicating that sorption occurs on two sites, one at low loadings and the other at high loadings within the concentration range of the experiments. Montmorillonite, the major component of bentonite, is known to sorb cations at surface sites as well as in the interlayer positions.

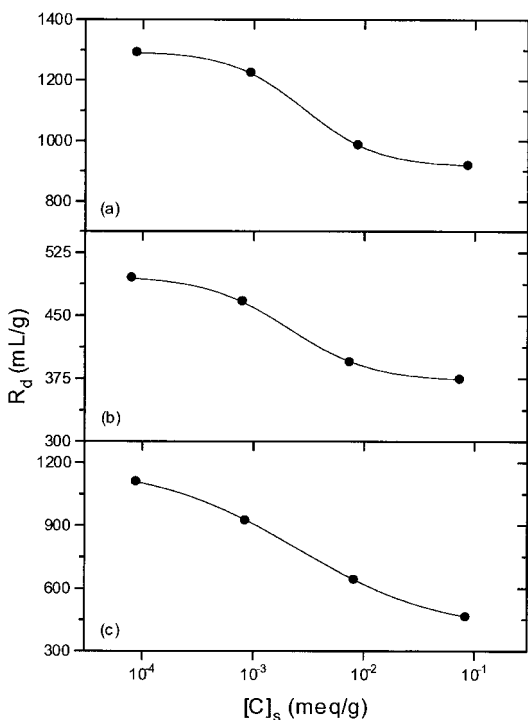


Fig. 2. The loading curves at  $T = 303$  K corresponding to sorption of: (a) Cs, (b) Ba, and (c) Co on bentonite.

Freundlich isotherms adequately described the sorption data of the three cations. The linear form of Freundlich equation is:

$$\ln[C]_s = \ln k + n \ln[C]_l \quad (2)$$

The terms  $[C]_s$  and  $[C]_l$  refer to the equilibrium concentration of the sorbed cation on solid and liquid phases, while  $k$  and  $n$  are constants. The values of  $n$  and  $k$  obtained from the slopes and intercepts of the least square fits are given in Table 1. The constant  $k$  provides quantitative information on the relative sorption affinity of the clay and the constant  $n$  characterizes the deviation of sorption from the linearity. The values of  $n$  being less than 1.0 in all cases indicate a non-linear sorption that takes place on a heterogeneous surface [3]. The  $k$  values indicate that bentonite possess the highest affinity toward Cs<sup>+</sup> sorption at lower temperatures. It is interesting to note that while the affinity of Cs<sup>+</sup> and Ba<sup>2+</sup> sorption decreased with increasing temperature, that of Co<sup>2+</sup> increased.

Empirical equations relating  $R_d$  values to  $[C]_l$  were developed utilizing the Freundlich parameters,  $n$  and  $k$ .  $R_d$  can be related to the equilibrium concentration,  $[C]_l$  utilizing Eq. (2):

$$R_d = k[C]_l^{n-1} \quad (3)$$

If the variations of  $k$  and  $n$  are expressed as a function of temperature, then the equation above would be helpful in predicting  $R_d$  values for various loading and temperature conditions. From Table 1, it is seen that while the values of  $n$  are nearly temperature independent, those of  $k$  vary with temperature. As a result the  $n$  values were expressed as the average of the entire temperature range. The  $k$  values were plotted as a function of temperature. Based on these,  $R_d$  may then be expressed as:

$$R_d = (a + bT)[C]_l^{\bar{n}-1} \quad (4)$$

Where  $a$  and  $b$  are constants,  $T$  is the temperature (K), and  $\bar{n}$  is the average of  $n$  values obtained from different temperatures. The values of the parameters found in this work are given in Table 2. The significance of Eq. (4) is the incorporation of the entire concentration ( $1 \times 10^{-3}$ – $1 \times 10^{-6}$  meq/ml) and temperature ( $30^\circ\text{C}$ – $60^\circ\text{C}$ ) ranges into the  $R_d$  values. The sorption data were also described well using the Dubinin–Radushkevich (D–R) isotherm model. The linear form of the D–R isotherm is:

$$\ln[C]_s = \ln C_m - K\varepsilon^2 \quad (5)$$

Table 1. Values of Freundlich constants,  $n$  and  $k$ , obtained from the linear fits of sorption data of Cs<sup>+</sup>, Ba<sup>2+</sup>, and Co<sup>2+</sup> on bentonite. (The Linear Correlation Coefficients were all greater than 0.998).

Temper. (K)	Cs-bentonite		Ba-bentonite		Co-bentonite	
	$n$	$k$	$n$	$k$	$n$	$k$
303	0.95	617	0.95	249	0.89	189
313	0.90	282	0.95	209	0.91	251
323	0.91	209	0.95	204	0.92	331
333	0.90	174	0.94	160	0.92	389

**Table 2.** The values of  $a$ ,  $b$ , and  $\bar{n}$  for the sorption of  $\text{Cs}^+$ ,  $\text{Ba}^{2+}$ , and  $\text{Co}^{2+}$  on bentonite.

	$a$	$b$	$\bar{n}$
Cs-bentonite	1965.9	-5.40	0.92
Ba-bentonite	1070.5	-2.72	0.95
Co-bentonite	-1872.4	6.80	0.91

Where  $\varepsilon$  is given as  $RT \ln(1 + 1/[C]_i)$ ,  $R$  is the ideal gas constant (8.3145 J/mol K),  $T$  is the absolute temperature (K),  $K$  is a constant related to sorption energy, and  $C_m$  refers to the sorption capacity of adsorbent per unit weight (meq/g). The parameters  $K$  and  $C_m$  were obtained from the least square fits to the data. The sorption energy,  $E$ , was calculated using  $K$  values from the relation:

$$E = (-2K)^{-0.5} \quad (6)$$

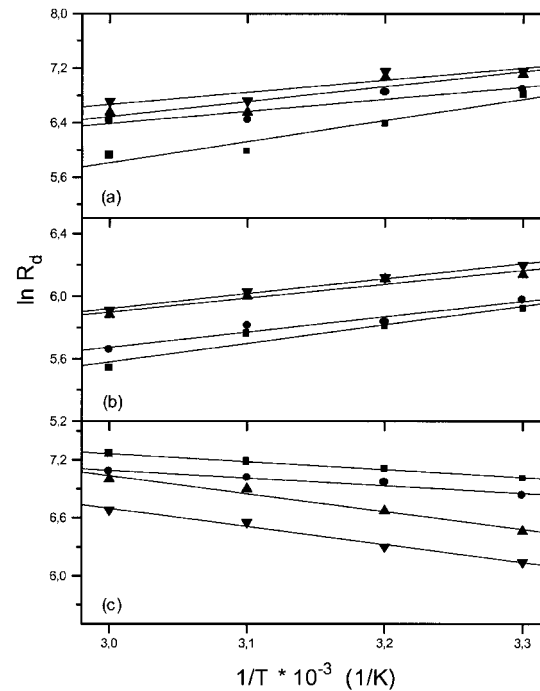
Here  $E$  refers to the amount of energy required to transfer one mole of sorbed ions from infinity in solution to the solid surface [4]. The values of  $C_m$ ,  $K$  and  $E$  obtained in this work are given in Table 3. The sorption capacity at lower temperatures is largest for  $\text{Cs}^+$  sorption. At higher temperatures the sorption capacity for  $\text{Co}^{2+}$  increases significantly. In all cases, the energy of sorption,  $E$ , is in the 8–16 kJ/mol energy range which corresponds to an ion-exchange type of sorption mechanism [5].

Utilizing the sorption data at different temperatures, the values of  $\Delta H^\circ$ ,  $\Delta S^\circ$ , and  $\Delta G^\circ$  of sorption were obtained using the equations:

$$\ln R_d = \frac{\Delta S^\circ}{R} - \frac{\Delta H^\circ}{RT} \quad (7)$$

$$\Delta G^\circ = \Delta H^\circ - T\Delta S^\circ \quad (8)$$

Plotting  $\ln R_d$  versus reciprocal temperature,  $\Delta H^\circ$  is obtained from the slope and  $\Delta S^\circ$  from the intercept. These values were then used in calculating  $\Delta G^\circ$  at different temperatures. The least square fits for  $\text{Cs}^+$ ,  $\text{Ba}^{2+}$ , and  $\text{Co}^{2+}$  sorption are shown in Fig. 3. Values of  $\Delta H^\circ$  and  $\Delta S^\circ$  and  $\Delta G^\circ$  are given in Table 4.  $\Delta H^\circ$  values were negative for  $\text{Cs}^+$  and  $\text{Ba}^{2+}$  and positive for  $\text{Co}^{2+}$  indicating exothermic

**Fig. 3.** Arrhenius plots ( $\ln R_d$  vs.  $1/T$ ) obtained for the sorption of: (a) Cs, (b) Ba, and (c) Co on bentonite at different initial concentrations (meq/ml). ■:  $1.0 \times 10^{-3}$  ●:  $1.0 \times 10^{-4}$  ▲:  $1.0 \times 10^{-5}$  ▼:  $1.0 \times 10^{-6}$ .

and endothermic nature of sorption, respectively. Thus, a decrease in temperature would favour sorption of  $\text{Cs}^+$  and  $\text{Ba}^{2+}$ , while a temperature increase enhances  $\text{Co}^{2+}$  sorption. Exothermic nature of  $\text{Cs}^+$  sorption was reported on a number of solids [6–8]. The endothermic behavior of  $\text{Co}^{2+}$  on some solids was reported in other studies [7, 9–11].  $\text{Co}^{2+}$  ions have high hydration energies and are well known for making aqua-hydrated cations in water. For cations that are highly solvated in water, adsorption requires that they be denuded of their hydration sheath so that their bonding to the sorption interface is facilitated. The dehydration process requires energy and this energy probably exceeds the bonding energy of the ions to the surface. The implicit assumption here is that after sorption, the metal ions are less hydrated than in solution. The removal of water from ions

**Table 3.** The D–R Isotherm constants,  $K$  (mol/kJ)<sup>2</sup> and  $C_m$  (meq/100 g) obtained from the least square fits to the sorption data of  $\text{Cs}^+$ ,  $\text{Ba}^{2+}$ , and  $\text{Co}^{2+}$  on bentonite and the mean free energy,  $E$  (kJ/mol) values obtained from  $K$  values. (The Linear Correlation Coefficients were all greater than 0.996).

Temp. (°K)	Cs-Bentonite			Ba-Bentonite			Co-bentonite		
	$K$	$C_m$	$E$	$K$	$C_m$	$E$	$K$	$C_m$	$E$
303	0.0057	158.1	9.4	0.0062	101.8	9.0	0.0056	100.1	9.4
313	0.0052	116.0	9.8	0.0058	90.1	9.3	0.0053	118.2	9.7
323	0.0051	94.6	9.9	0.0055	93.9	9.5	0.0049	115.6	10.1
333	0.0048	91.6	10.2	0.0052	78.9	9.8	0.0046	136.5	10.4

**Table 4.** The enthalpy change,  $\Delta H^\circ$  (kJ/mol), the entropy change,  $\Delta S^\circ$  (J/mol K), and the Gibbs free energy change,  $\Delta G^\circ$  (kJ/mol) obtained from the sorption data of  $\text{Cs}^+$ ,  $\text{Ba}^{2+}$ , and  $\text{Co}^{2+}$  on bentonite.

	Cs-bentonite	Ba-bentonite	Co-bentonite
$\Delta H^\circ \pm \text{S.D.}$ (kJ/mol)	-19 ± 4	-8 ± 1	11 ± 4
$\Delta S^\circ \pm \text{S.D.}$ (J/mol K)	-3 ± 1	23 ± 4	90 ± 10
$\Delta G^\circ \pm \text{S.D.}$ (kJ/mol)	-18 ± 1	-16 ± 1	-17 ± 2

is essentially an endothermic process, and as more heat is supplied by increasing the temperature of adsorption, more dehydrated cations will be available and thus the extent of sorption is expected to increase [12].

Positive  $\Delta S^\circ$  values were obtained for Ba<sup>2+</sup> and Co<sup>2+</sup> sorption. In literature, it is reported that the positive values of  $\Delta S^\circ$  for sorption of divalent cations (Ba<sup>2+</sup> and Co<sup>2+</sup> in this case) on solid surfaces might be suggesting that ions displaced from the solid surface are greater in number than the sorbed Ba<sup>2+</sup> or Co<sup>2+</sup> ions, which means that two monovalent ions may be exchanged for a single Ba<sup>2+</sup> or Co<sup>2+</sup> ion [7]. The negative values of  $\Delta G^\circ$  for all cases indicate that the sorption process is spontaneous while the magnitudes are close to the 8–16 kJ/mol energy range which corresponds to ion exchange type sorption mechanism [5].

### ToF-SIMS studies

ToF-SIMS technique enabled the study of Cs<sup>+</sup>, Ba<sup>2+</sup>, and Co<sup>2+</sup> sorption across the surface of bentonite in addition to the extent of depletion of exchanged cations within the clay matrix. In addition to analysis of the uppermost surface, depth profiling up to 70 Å was performed. Bentonite samples contained initially the major elements Si, Al, Fe, Mg, Na with corresponding atomic percentages of 60.4, 18.8, 14.4, 4.1, 1.6, respectively in addition to minor amounts of K, Ca, and Li with a total percentage of 0.7. The sensitivity factor-corrected data were expressed relative to (Al+Si), assuming that both are nonexchanging cations. The Na<sup>+</sup> and Mg<sup>2+</sup> contents in the clay structure decreased significantly upon sorption of Cs<sup>+</sup>, Ba<sup>2+</sup>, and Co<sup>2+</sup> ions. The extent of decrease of cation,  $x$ , following sorption may be represented

by a ‘depletion factor’, DF, defined as:

$$(DF)_x = \frac{(R_i)_x - (R_f)_x}{(R_i)_x} \quad (9)$$

Here  $(R_i)_x$  and  $(R_f)_x$  are the cation/(Si+Al) ratio of cation  $x$  prior to and following sorption, respectively. The magnitude of DF is related to the affinity of cation  $x$  towards exchange with the sorbed ion. Its highest value of unity indicates complete exchange and lowest value of zero indicates no exchange. Fig. 4a,b give DF's of Na<sup>+</sup> and Mg<sup>2+</sup>, plotted against depth in the bentonite lattice. In all cases, Na<sup>+</sup> showed higher DF values than Mg<sup>2+</sup>, indicating a higher exchange affinity. The depleted amount of a cation  $x$  is calculated by multiplying the difference  $[(R_i)_x - (R_f)_x]$  by  $z_x$ , the charge of cation  $x$ . This may be defined as the Equivalent Depleted Amount (EDA) of a particular cation. The percentage contribution of cation  $x$  to the total exchange ( $D_x$ ) of all cations at a given depth is then given as:

$$D_x = \frac{[(R_i)_x - (R_f)_x] \cdot z_x}{\sum_x \{[(R_i)_x - (R_f)_x] \cdot z_x\}_n} \times 100 \quad (10)$$

Table 5 gives the EDA and  $D_x$  values for Na<sup>+</sup> and Mg<sup>2+</sup>. While the total contribution of these ions to the exchange of Cs<sup>+</sup> and Ba<sup>2+</sup> is comparable, Mg<sup>2+</sup> contribution significantly surpasses that of Na<sup>+</sup> in the case of Co<sup>2+</sup> sorption.

The amounts of Cs<sup>+</sup>, Ba<sup>2+</sup>, and Co<sup>2+</sup> ions sorbed on bentonite as a function of matrix depth are plotted in Fig. 5. If the EDA of Na<sup>+</sup> and Mg<sup>2+</sup> are compared with the sorbed equivalents of Cs<sup>+</sup>, Ba<sup>2+</sup>, and Co<sup>2+</sup> (see Table 5), a significant difference is observed only in the case of Ba<sup>2+</sup> sorption. This suggests that in addition to

**Table 5.** The initial and final ratios of cation/(Al+Si),  $R_i$  and  $R_f$ , the Equivalent Depleted Amounts (EDA), and the percentage contribution to total depletion,  $D_x$ , as a function of depth for the sorption of Cs<sup>+</sup>, Ba<sup>2+</sup>, and Co<sup>2+</sup> on bentonite. All calculations are based on ToF-SIMS measurements.

Cation	Depth(A)	Cs-bentonite				Ba-bentonite				Co-bentonite	
		$R_i$	$R_f$	EDA	$D_x$	$R_f$	EDA	$D_x$	$R_f$	EDA	$D_x$
Na <sup>+</sup>	0	0.0419	0.0049	0.0370	62.29	0.0017	0.0402	96.17	0.0002	0.0417	50.67
	10	0.0309	0.0024	0.0285	60.51	0.0026	0.0283	37.88	0.0008	0.0301	30.87
	20	0.0221	0.0019	0.0202	44.49	0.0026	0.0195	32.77	0.0005	0.0216	23.18
	30	0.0165	0.0016	0.0149	37.16	0.0023	0.0142	42.77	0.0005	0.0161	19.24
	40	0.0125	0.0015	0.0110	35.71	0.0025	0.0100	32.26	0.0005	0.0120	17.00
	50	0.0102	0.0016	0.0086	47.78	0.0024	0.0078	24.68	0.0004	0.0098	14.89
	70	0.0016	0.0016	0.0070	34.65	0.0026	0.0060	18.40	0.0004	0.0082	12.46
Total				0.1272			0.1260			0.1395	
Mg <sup>2+</sup>	0	0.0456	0.0344	0.0224	37.71	0.0448	0.0016	3.83	0.0253	0.0406	49.33
	10	0.0546	0.0453	0.0186	39.49	0.0314	0.0464	62.12	0.0209	0.0674	69.13
	20	0.0556	0.0430	0.0252	56.51	0.0356	0.0400	67.23	0.0198	0.0716	76.82
	30	0.0544	0.0418	0.0252	62.84	0.0354	0.0190	57.23	0.0206	0.0676	80.76
	40	0.0504	0.0405	0.0198	64.29	0.0399	0.0210	67.74	0.0211	0.0586	83.00
	50	0.0487	0.0440	0.0094	52.22	0.0368	0.0238	75.32	0.0207	0.0560	85.11
	70	0.0496	0.0430	0.0132	65.35	0.0363	0.0266	81.60	0.0208	0.0576	87.54
Total				0.1338			0.1784			0.4194	
Cs <sup>+</sup>				0.3400							
Ba <sup>2+</sup>							0.8154				
Co <sup>2+</sup>										0.5316	

ion exchange with  $\text{Na}^+$  and  $\text{Mg}^{2+}$ , other sorption types (like surface complexation, site specific sorption, precipitation, etc.) might be taking place as complementary mechanisms.

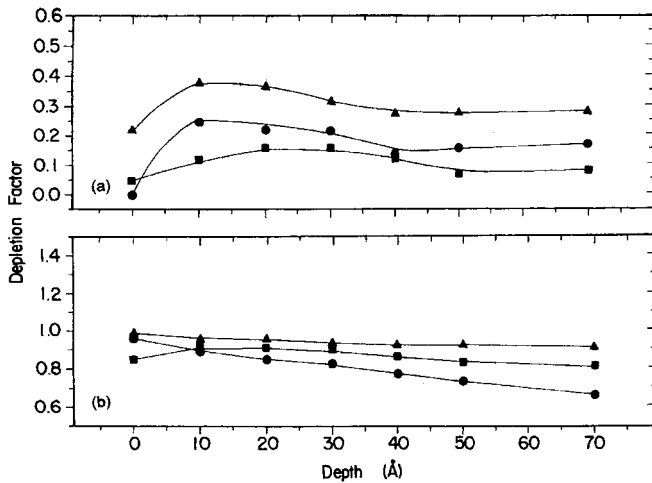


**Fig. 4.** The depletion factors of (a) Mg and (b) Na for sorption of  $\text{Cs}^+$ ,  $\text{Ba}^{2+}$ , and  $\text{Co}^{2+}$  on bentonite. ■: Cs-bentonite ●: Ba-bentonite ▲: Co-bentonite.

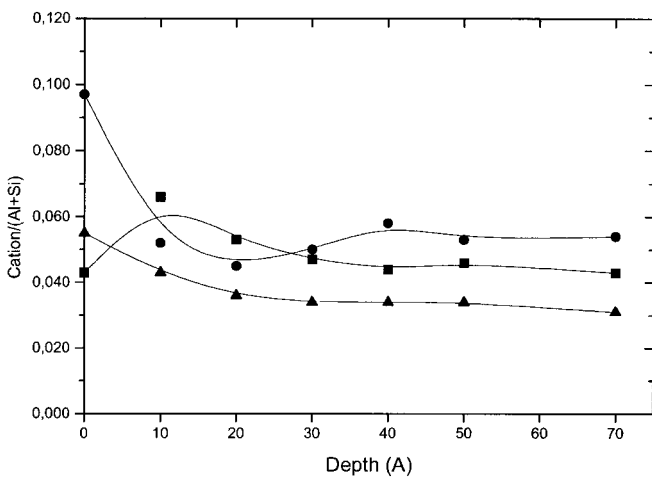


**Fig. 5.** The amounts (cation/(Al+Si)) of the sorbed  $\text{Cs}^+$ ,  $\text{Ba}^{2+}$ , and  $\text{Co}^{2+}$  as a function of depth (Å) in bentonite lattice. ■: Cs ●: Ba ▲: Co.

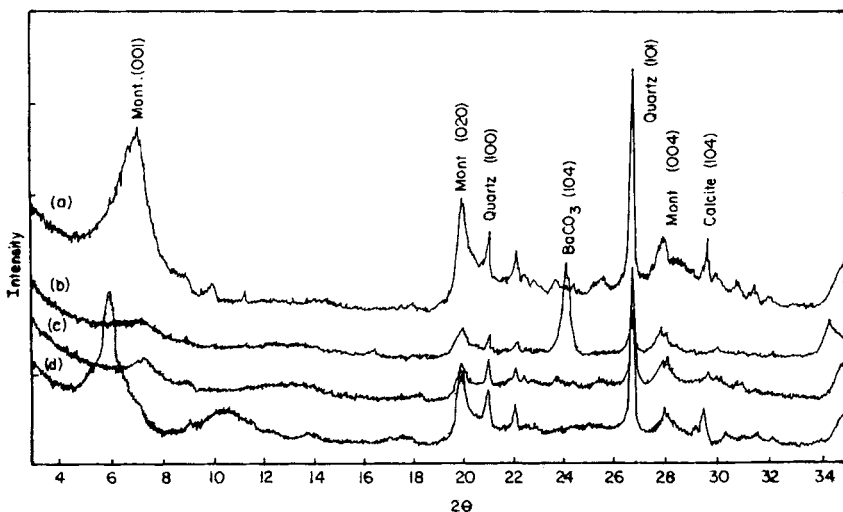


**Fig. 6.** XRD spectra of: (a) natural bentonite, (b) Ba-bentonite, (c) Cs-bentonite, and (d) Co-bentonite.

## X-ray diffraction (XRD) studies

In addition to the characterization of the clay samples, XRD was used to examine any structural changes on bentonite that accompanied the sorption of  $\text{Cs}^+$ ,  $\text{Ba}^{2+}$ , and  $\text{Co}^{2+}$ . The results showed (Fig. 6b,c,d) that while no major changes were observed in the case of  $\text{Cs}^+$  and  $\text{Co}^{2+}$  sorption, new features appeared in the  $\text{Ba}^{2+}$  sorbed samples. These were identified as  $\text{BaCO}_3$  with the major peak appearing at  $d_{hkl} = 3.696$ . The formation of  $\text{BaCO}_3$  have most probably taken place as a result of  $\text{Ba}^{2+}$  exchange with  $\text{Ca}^{2+}$  in the calcite matrix which existed in minor quantities in the bentonite samples.

*Acknowledgment.* We would like to thank G. C. Allen, L. Black, and K. R. Hallam at Bristol University for their help in ToF-SIMS and XRD measurements.

## References

1. Takahashi, M., Muroi, M., Inoue, A., Aoki, M., Takizawa, M., Ishigure, K., Fujita, N.: Properties of bentonite clay as buffer material in high-level geological disposal. Part I: chemical species in bentonite. *Nucl. Technol.* **76**, 221 (1987).
2. Wilson, M. J.: *Clay Mineralogy*. Chapman and Hall, New York 1994, p. 21.
3. Mishra, S. P., Tiwary D.: Ion exchangers in radioactive waste managements. *J. Radioanal. Nucl. Chem.* **196/2**, 353 (1995).
4. Aksoyoglu, S.: Sorption of U(VI) on granite. *J. Radioanal. Nucl. Chem.* **134(2)**, 393 (1989).
5. Helferrich, F.: *Ion Exchange*. Mc Graw Hill, New York 1962.
6. Oscarson, D. W., Watson, R. L., Miller, H. G.: The interaction of trace levels of cesium with monmorillonite and illite clays. *App. Clay Sci.* **2**, 29 (1987).
7. Khan S. A., Reman, R., Khan, M. A.: Sorption of Cs(I), Sr(II), and Co(II) on  $\text{Al}_2\text{O}_3$ . *J. Radioanal. Nucl. Chem.* **190**, 81 (1995).
8. Shahwan, T., Suzer, S., Erten, H. N.: Sorption studies of  $\text{Cs}^+$  and  $\text{Ba}^{2+}$  cations on magnesite. *Appl. Radiat. Isot.* **49/8**, 915 (1998).
9. Kwang, K., Kun-Jai, L., Jae-Heum, B.: Characterization of cobalt adsorption on prepared  $\text{TiO}_2$  and Fe-Ti-O adsorbents in high temperature water. *Separ. Sci. Tech.* **30/6**, 963 (1995).
10. Khan, S. A., Reman, R. U., Khan, M. A.: Sorption of cobalt on bentonite. *J. Radioanal. Nucl. Chem.* **207/1**, 19 (1996).
11. Shahwan, T., Erten, H. N.: Radiochemical study of  $\text{Co}^{2+}$  sorption on chlorite and kaolinite. *J. Radioanal. Nucl. Chem.* **241/1**, 151 (1999).
12. Qadeer, R., Hanif, J., Saleem, M., Afzal, M.: Surface characterization and thermodynamics of adsorption of  $\text{Sr}^{2+}$ ,  $\text{Ce}^{3+}$ ,  $\text{Sm}^{3+}$ ,  $\text{Cd}^{3+}$ ,  $\text{Th}^{4+}$ ,  $\text{UO}_2^{3+}$  on activated charcoal from aqueous solution. *Colloid. Polym. Sci.* **271**, 83 (1993).